REPORT DOCUMENTATION PAGE

Form Approved

OMB No. 0704-0188

The public reporting burden for this collection of information is estimated to average 1 hour per response, including the time for reviewing instructions, searching existing data sources, gathering and maintaining the data needed, and completing and reviewing the collection of information. Send comments regarding this burden estimate or any other aspect of this collection of information, including suggestions for reducing the burden, to Department of Defense, Washington Headquarters Services, Directorate for Information Operations and Reports (0704-0188), 1215 Jefferson Davis Highway, Suite 1204, Arlington, VA 22202-4302. Respondents should be aware that notwithstanding any other provision of law, no person shall be subject to any penalty for failing to comply with a collection of information if it does not display a currently valid OMB control number.

PLEASE DO NOT RETURN YOUR FORM TO THE ABOVE ADDRESS.

1. REPORT DATE *(DD-MM-YYYY)*	2. REPORT TYPE	3. DATES COVERED *(From - To)*
11-08-2015	Final	29 Sep 2014 – 28 Mar 2015

4. TITLE AND SUBTITLE

Autonomous soft landing of aerospace vehicles

5a. CONTRACT NUMBER
FA2386-14-1-4103

5b. GRANT NUMBER
Grant 14IOA125_114103

5c. PROGRAM ELEMENT NUMBER
61102F

6. AUTHOR(S)

Assoc. Prof. Radhakant Padhi

5d. PROJECT NUMBER

5e. TASK NUMBER

5f. WORK UNIT NUMBER

7. PERFORMING ORGANIZATION NAME(S) AND ADDRESS(ES)

Indian Institute of Science
Bangalore 560-012
India

8. PERFORMING ORGANIZATION REPORT NUMBER

N/A

9. SPONSORING/MONITORING AGENCY NAME(S) AND ADDRESS(ES)

AOARD
UNIT 45002
APO AP 96338-5002

10. SPONSOR/MONITOR'S ACRONYM(S)

AFRL/AFOSR/IOA(AOARD)

11. SPONSOR/MONITOR'S REPORT NUMBER(S)

14IOA125_114083

12. DISTRIBUTION/AVAILABILITY STATEMENT

Distribution Code A: Approved for public release, distribution is unlimited.

13. SUPPLEMENTARY NOTES

14. ABSTRACT

Two vertical soft landing problems are investigated in this report. First, the soft landing problem of quadrotor in presence of unmodelled dynamics is investigated. A neural network-based disturbance estimation is adopted to capture the unmodeled quadrotor dynamics due to rotor blade flapping phenomenon. An adaptive guidance law with the Dynamic Inversion (DI) as baseline algorithm is illustrated for soft vertical touch down. Next, the autonomous landing of a spacecraft on the lunar surface is explored. To ensure the smooth touchdown of the spacecraft on the lunar surface, a nonlinear optimal control theory based Generalized model predictive static programming (G-MPSP) guidance is proposed. As the G-MPSP formulation incorporates the terminal condition as a hard constraint, it ensures the high terminal accuracy of position and velocity of the spacecraft. Also the vertical orientation of the spacecraft during touchdown is achieved through the soft constraint formulation by the proper selection of the control weight matrix. Effectiveness of the proposed guidance methods are demonstrated using simulation results.

15. SUBJECT TERMS

Control Theory, Optimal Control

16. SECURITY CLASSIFICATION OF:			17. LIMITATION OF ABSTRACT	18. NUMBER OF PAGES	19a. NAME OF RESPONSIBLE PERSON
a. REPORT	b. ABSTRACT	c. THIS PAGE			Ingrid J. Wysong, Ph.D.
U	U	U	SAR	47	19b. TELEPHONE NUMBER *(Include area code)* +81-42-511-2000

Report Documentation Page

Form Approved
OMB No. 0704-0188

Public reporting burden for the collection of information is estimated to average 1 hour per response, including the time for reviewing instructions, searching existing data sources, gathering and maintaining the data needed, and completing and reviewing the collection of information Send comments regarding this burden estimate or any other aspect of this collection of information, including suggestions for reducing this burden, to Washington Headquarters Services, Directorate for Information Operations and Reports, 1215 Jefferson Davis Highway, Suite 1204, Arlington VA 22202-4302 Respondents should be aware that notwithstanding any other provision of law, no person shall be subject to a penalty for failing to comply with a collection of information if it does not display a currently valid OMB control number

1. REPORT DATE	2. REPORT TYPE	3. DATES COVERED
11 AUG 2015	**Final**	**29-09-2014 to 28-09-2015**

4. TITLE AND SUBTITLE	5a. CONTRACT NUMBER
Autonomous soft landing of aerospace vehicles	**FA2386-14-1-4103**
	5b. GRANT NUMBER
	5c. PROGRAM ELEMENT NUMBER **61102F**
6. AUTHOR(S) **Radhakant Padhi**	5d. PROJECT NUMBER
	5e. TASK NUMBER
	5f. WORK UNIT NUMBER
7. PERFORMING ORGANIZATION NAME(S) AND ADDRESS(ES) **Indian Institute of Science,Bangalore 560-012,India,NA,NA,NA**	8. PERFORMING ORGANIZATION REPORT NUMBER **N/A**
9. SPONSORING/MONITORING AGENCY NAME(S) AND ADDRESS(ES) **AOARD, UNIT 45002, APO, AP, 96338-5002**	10. SPONSOR/MONITOR'S ACRONYM(S) **AFRL/AFOSR/IOA(AOARD)**
	11. SPONSOR/MONITOR'S REPORT NUMBER(S) **14IOA125_114083**

12. DISTRIBUTION/AVAILABILITY STATEMENT
Approved for public release; distribution unlimited

13. SUPPLEMENTARY NOTES

14. ABSTRACT

Two vertical soft landing problems are investigated in this report. First, the soft landing problem of quadrotor in presence of unmodelled dynamics is investigated. A neural network-based disturbance estimation is adopted to capture the unmodeled quadrotor dynamics due to rotor blade flapping phenomenon. An adaptive guidance law with the Dynamic Inversion (DI) as baseline algorithm is illustrated for soft vertical touch down. Next, the autonomous landing of a spacecraft on the lunar surface is explored. To ensure the smooth touchdown of the spacecraft on the lunar surface, a nonlinear optimal control theory based Generalized model predictive static programming (G-MPSP) guidance is proposed. As the G-MPSP formulation incorporates the terminal condition as a hard constraint, it ensures the high terminal accuracy of position and velocity of the spacecraft. Also the vertical orientation of the spacecraft during touchdown is achieved through the soft constraint formulation by the proper selection of the control weight matrix. Effectiveness of the proposed guidance methods are demonstrated using simulation results.

15. SUBJECT TERMS
Control Theory, Optimal Control

16. SECURITY CLASSIFICATION OF:			17. LIMITATION OF ABSTRACT	18. NUMBER OF PAGES	19a. NAME OF RESPONSIBLE PERSON
a REPORT **unclassified**	b ABSTRACT **unclassified**	c THIS PAGE **unclassified**	**Same as Report (SAR)**	**47**	

Guidance of Autonomous Aerospace Vehicles for Vertical Soft Landing using Nonlinear Control Theory

Report No. IISc/CSIC/AE/RP/AOARD/2015/01

Girish Joshi, Kapil Sachan, Avijit Banerjee, Radhakant Padhi

Department of Aerospace Engineering

Indian Institute of Science

Bangalore, 560012, INDIA

Distribution Code A: Approved for public release, distribution is unlimited

Abstract

Two vertical soft landing problems are investigated in this report. First, the soft landing problem of quadrotor in presence of unmodelled dynamics is investigated. A neural network based disturbance estimation is adopted to capture the unmodeled quadrotor dynamics due to rotor blade flapping phenomenon. An adaptive guidance law with the Dynamic Inversion (DI) as baseline algorithm is illustrated for soft vertical touch down. Next, the autonomous landing of a spacecraft on the lunar surface is explored. To ensure the smooth touchdown of the spacecraft on the lunar surface, a nonlinear optimal control theory based Generalized model predictive static programming (G-MPSP) guidance is proposed. As the G-MPSP formulation incorporates the terminal condition as a hard constraint, it ensures the high terminal accuracy of position and velocity of the spacecraft. Also the vertical orientation of the spacecraft during touchdown is achieved through the soft constraint formulation by the proper selection of the control weight matrix. Effectiveness of the proposed guidance methods are demonstrated using simulation results.

Distribution Code A: Approved for public release, distribution is unlimited

Contents

Distribution Code A: Approved for public release, distribution is unlimited

Distribution Code A: Approved for public release, distribution is unlimited

List of Figures

Distribution Code A: Approved for public release, distribution is unlimited

Distribution Code A: Approved for public release, distribution is unlimited

0.1 Introduction

In general the objective of the guidance algorithm for the autonomous vertical soft landing of a UAV is to ensure that it touches down at the designated site vertically with near-zero vertical velocity. Near-zero touchdown velocity is essential for the safety of the vehicle as well the on-board payload/instrument. The desired lading site comes from the mission requirement. During landing it is also essential to maintain the vertical orientation of the vehicle with respect to ground. To avoid the local uneven surface of desired landing site it might be necessary to shift the landing site location to a nearby smooth ground. Such requirements may comes from the vision based information and the necessary correction for the trajectory needs to be recomputed online. Two related but different problems (which offer different challenges) are investigated in this report. One problem deals with the quadrotor UAV which needs to land on earth surface in presence of modelling uncertainty and another deals with soft landing on the surface of the moon.

Quadrotor UAVs are emerging as popular choice as both experimental research platform and for commercial use. Due to their design and construction simplicity, vertical take off and landing, hovering capability and ease of operation within confined spaces, capability to do aggressive maneuvers quadrotors are preferred over winged UAV. Quadrotor utilizes lift generated from four propellers blades for the lateral, longitudinal and altitude control. Unlike conventional helicopters which utilizes a tail rotor for controlling body spin resulting from angular momentum conservation of the rotor blades, quadrotor does not need a tail rotor since opposite rotor blade pair rotate in opposite direction and hence counteracting each others angular momentum, this feature makes quadrotors yet more reliable over helicopters. For detailed operation, functional details of quadrotor system one can refer Beard [2008].

After 1963, the first manned flight (hovering) of the four rotor configuration of quadrotor helicopter by Cutis-Wright X19A no much advancement was seen in the multi-rotor flight due to stability issues due actuator dissimilarities which lead to instability in the quad flight, rendering stable flight nearly impossible. With recent advancement of the micro-controller

Distribution Code A: Approved for public release, distribution is unlimited

and solid state electronics the onboard computer has become more smaller and faster Hartley et al. [2013]. With availability of small, light, high fidelity sensors (Inertial Measurement Units IMU) and processors on board, advanced controls for quadrotor have become a reality. Many research teams have proposed various control architectures for quadrotor control and guidance. Most popular control experimented on quadrotor UAV platform are linear feedback control architecture like PID, LQR Huang et al. [2009], Pounds et al. [2010]etc. For indoor and low speed flight fixed gain linear feedback controller are quite capable of delivering the requisite performance of attitude control and trajectory tracking. Since linear control utilizes the linearized plant dynamics model for control computation, under scenario like parameter uncertainty viz inertia change or partial actuator failure, under influence of un-modeled plant dynamics or under external perturbation these controller fail to achieve the required performance. Many research group have demonstrated the command trajectory tracking for indoor flights and formation flight like OS4 quadrotor project Bouabdallah et al. [2005], MIT SWARM Valenti et al. [2006] and at Stanford Testbed of Autonomous Rotorcraft for Multi-Agent Control (STARMAC) Huang et al. [2009], Hoffmann et al. [2007]. Several adaptive control techniques are also experimented as well in quadrotor control, Annaswamy et al. have experimented MRAC based controller in presence of actuator uncertainties Dydek et al. [2010] and Whitehead and Bieniaswski Whitehead and Bieniawski [2010] have demonstrated MRAC controller for step command in altitude tracking under actuator degradation. Chowdhary et al. Chowdhary et al. [2012] have experimented and presented concurrent learning MRAC for outer-loop control and PD based controller for attitude controller of quad-rotor where the gains are tuned for larger quad-rotor frame and same control gains are ported to much smaller quad-rotor for trajectory tracking problem. Gabriel Hoffman et al. have experimented PD controller with integral feedback controller catering for blade flapping uncertainty. Integral feedback control accounts for this uncertainty as a constant bias i.e. for uncertainty at constant velocity and attitude angle, but as the vehicle velocity and attitude changes the integral control has to adapt to new uncertain moment values. In the problem experimented in this paper for commanded spiralling trajectory tracking this control architecture will fail to perform the desired tracking, hence there is need for controller which adapts online to approximate the uncertainty for control computation. Similarly Pounds et al. Pounds et al. [2010] have experimented linear PID and LQR based controller compensating for uncertainty due to blade flapping phenomenon.

Distribution Code A: Approved for public release, distribution is unlimited

But as per authors knowledge not many have experimented on adaptive control catering for aerodynamic uncertainty in trajectory tracking.

This report proposes a control architecture utilizing the well-established Dynamic Inversion(DI) theory and augmenting it with online trained Radial Basis Function (RBF) neural networks a robust nonlinear controller catering to the actual plant model is experimented and results are presented in this article. This control architecture is experimented with plant model of Quadrotor trajectory tracking problem.The RBF-NN is used to capture the unmodeled dynamics/uncertainty in the system due to rotor blade flapping phenomenon. A new weight update rule based adaptive controller with DI as baseline controller is validated for quadrotor trajectory tracking problem. It is observed that proposed controller is able to capture the time varying uncertainty perfectly and thereby augmenting the approximate system dynamics to track the actual system dynamics. The DI control evaluated using online augmented approximate plant, satisfactorily tracks the commanded attitude angles and hence achieving the desired trajectory tracking through outer-loop control. The details are presented in the subsequent results section.

Distribution Code A: Approved for public release, distribution is unlimited

1 Control Synthesis: Generic Theory

In this section the methodology used for autonomous guidance for soft landing is described with necessary mathematical details.

1.1 Philosophy of Adaptive Dynamic Inversion

This section gives the details of the philosophy of the online adaption method of DI controller. A online trained NN is used along with the inner loop DI controller of the quad-rotor to capture the plant disturbance, update the plant model and there by synthesizing the over all controller. RBF-NN approximates the un-modeled dynamics which is crucial for online adaptation of DI controller. The approximate model synthesized using trained NN, is termed as a modified state observer Joshi and Padhi [2013]. NNs use the channel wise error information in the state for training, single layer networks are employed with radial basis function as basis vectors. The nominal plant model which is fully known is assumed to have the following structure

$$\dot{X} = f_0(X) + g(X)U \tag{1.1}$$

where $X \in \Re^n$; $U \in \Re^m$ and $y \in \Re^p$, $f_0(X)$ and $g(X)$ represents nominal system. Nominal controller U is designed such that the states of nominal plant model X track the respective states of the desired plant (1.4) i.e. goal is to ensure that $X \to X_d$ as $t \to \infty$.

Distribution Code A: Approved for public release, distribution is unlimited

The actual system or actual plant model is considered as to be having a structure

$$\dot{X} = f(X) + g(X)U + d_{ext}(X) \tag{1.2}$$

where $f(X)$ is actual system model, $d_{ext}(X)$ denotes the disturbance external to the system. Since the actual system parameters are unknown and external disturbance model is uncertain, the actual plant model cannot be used for control synthesis.
The total system uncertainty can therefore be denoted by the term $d(X) = (f(X) - f_0(X) + d_{ext}(X))$, where $d(X) \in \Re^n$ represents the total uncertainty term in the system (1.2). The uncertain actual plant model can be represented using nominal plant model and uncertainty term $d(X)$ as follows

$$\dot{X} = f_0(X) + g(X)U + d(X); \quad y = h(X) \tag{1.3}$$

Consider a nonlinear systems representation for the desired plant dynamics. The desired plant dynamics output the desired state trajectory for the actual system to follow

$$\dot{X}_d = f_d(X_d) \tag{1.4}$$

where $X_d \in \Re^n$ represents the desire state vector.
In the actual plant model (1.3) the term $d(X)$ is unknown, the objective is to first capture the unknown function $d(X)$ through NN approximation $\hat{d}(X) = W^T\Phi(X)$ and form an approximate system model as follows.

$$\dot{X}_a = f_0(X) + g(X)U + \hat{d}(X) + K_\tau(X - X_a) \tag{1.5}$$

Concept of modified state observer is applied with DI to form the actual controller. The controller synthesis call for two step process for control realization

1. $X \to X_a$ as $t \to \infty$. The complete state feedback is not available but reduced order state vector X_{meas} is available through the state measurement. The measured state values

Distribution Code A: Approved for public release, distribution is unlimited

are considered to be corrupted by measurement noise and can be represented as

$$X_{meas} = y + \mathcal{N}(0, \sigma^2)$$

where σ represents the standard deviation of the zero mean white noise. Hence the revised the aim is to ensure

$$X_{est} \rightarrow X_a$$

where X_{est} is the Extended Kalman filter estimate of the state vector X. Using estimated state value, the approximate plant model is written as

$$\dot{X}_a = f_0(X_{est}) + g(X_{est})U + \hat{d}(X_{est}) + K_\tau(X_{est} - X_a) \tag{1.6}$$

2. $X_a \rightarrow X_d$ as $t \rightarrow \infty$: This process is accomplished through control synthesis using online adaptation of DI controller.

1.1.1 Control Synthesis using Feed-Back Linearization Method

For the control synthesis it is considered that the unknown function $\hat{d}(X_{est})$ is function of X_{est} and not X since the uncertainty approximation available through RBF-NN and the RBF basis is function of X_{est}.

$$\Phi(X_{est}) = e^{\left(\frac{1}{2\sigma^2}|X_{est}-C|^2\right)} \tag{1.7}$$

With the objective of the controller to enforce $X_a \rightarrow X_d$. The plant dynamics for Feedback Linearization control synthesis can be written as follows,

$$\ddot{X}_a = \nu \tag{1.8}$$

where ν is termed as synthetic control to linearized plant model (1.8). Any linear control technique can be implemented to evaluate the linear synthetic control term ν. In this paper a Linear Quadratic Regulator(LQR) technique is used for control computation. Once the synthetic controller ν is evaluated the expression for the actual controller of the plant U can be evaluated by inverting the plant dynamics. Inverting and simplifying the above approximate

Distribution Code A: Approved for public release, distribution is unlimited

plant dynamics (1.6) the expression for control U can be written as

$$U = \left[g(X_{est})\right]^{-1}(\nu - f_0(X_{est}) - \hat{d}(X_{est}) - K_\tau(X_{est} - X_a)) \tag{1.9}$$

This closed form expression for control U is valid provided $\left[g(X_{est})\right]^{-1}$ exists for all values X_{est}. In particular for the quad-rotor plant considered in this paper $g(X_{est})$ is a product of inverse of rotation matrix and inertia matrix for the quad frame. Since both the matrix are invertible at all times except when roll and pitch attitude of vehicle i.e. $\phi, \theta = 90^0$ the closed form expression for control (1.9) is valid for all other domain of operation.

1.1.2 Neural Network Synthesis and Weight Update Rule

The single layer NN is designed to capture the un-modeled dynamics of the plant. It is desired that virtual (approximate) plant model should track the actual plant. Error term between actual (X) and virtual states vector (X_a) can be defined as

$$E = X - X_a \tag{1.10}$$

Since the actual state vector X is not available instead a EKF estimate is used, note that here we introduce a small abuse of notation in this section, state vector X denotes the EKF estimate of the state vector. The error dynamics can be obtained by differentiating the above equation with time and substituting for $\dot{X}$ and $\dot{X}_a$ from (1.3) and (1.5)

$$\begin{aligned} \dot{E} &= \dot{X} - \dot{X}_a \\ \dot{E} &= d(X) - \hat{d}(X) - K_\tau E \end{aligned} \tag{1.11}$$

Single layer NN with RBF basis functions is chosen to approximates the un-modeled dynamics $d_i(X)$ in the i^{th} channel.

$$\hat{d}_i(X) = \hat{W}_i{}^T \Phi_i(X),\ W_i \in \Re^p \tag{1.12}$$

where, $\hat{W}_i$ are the actual weights and $\Phi_i(X)$ are the basis function. Lets consider there exists an ideal approximator for the unknown function which approximates $d_i(X)$ with an ideal

Distribution Code A: Approved for public release, distribution is unlimited

approximation error ϵ_i for the chosen basis $\Phi_i(X)$.

$$d_i(X) = {W_i}^T \Phi_i(X) + \epsilon_i \tag{1.13}$$

The weights W_i are the ideal weights which are unknown. Channel wise error dynamics can be written as

$$\dot{e}_i = {W_i}^T \Phi_i(X) + \epsilon_i - {\hat{W}_i}^T \Phi_i(X) - k_{\tau_i} e_i \tag{1.14}$$

The error in weights of the i^{th} approximating network is defined as

$$\tilde{W}_i = W_i - \hat{W}_i \tag{1.15}$$

$$\dot{\tilde{W}}_i = -\dot{\hat{W}}_i, \quad W_i = constant \tag{1.16}$$

Aim is that weights of the approximating networks $\hat{W}_i$ should approach the ideal weights W_i asymptotically, i.e.,

$$\tilde{W}_i \to 0 \ \ as \ \ t \to \infty$$

The un-modeled information is stored in terms of the weights of the approximating networks. Lyapunov based approach for deriving weight update rule is discussed in the next subsection for updating $\hat{W}_i$ online.

Weight Update Rule

The candidate Lyapunov function ensures the asymptotic stability of the following variables, channel wise error e_i, error in network weights $\tilde{W}_i$ and error in gradient of disturbance term (for directional learning)

$$\left[\frac{\partial d_i(X)}{\partial X} - \frac{\partial \hat{d}_i(X)}{\partial X} \right] = \tilde{{W_i}^T} \left[\frac{\partial \Phi_i}{\partial X} \right] \tag{1.17}$$

A positive definite Lyapunov function candidate function is selected as follows

$$V_i(e_i, \tilde{W}_i) = \beta_i \frac{e_i^2}{2} + \frac{\tilde{{W_i}^T} \tilde{W}_i}{2\gamma_i} + \tilde{{W_i}^T} \left[\frac{\partial \Phi_i}{\partial X} \right] \frac{\Theta_i}{2} \left[\frac{\partial \Phi_i}{\partial X} \right]^T \tilde{W}_i \tag{1.18}$$

Distribution Code A: Approved for public release, distribution is unlimited

where, β_i, γ_i and Θ_i are positive definite quantities. Taking time derivative of Lyapunov function and substituting the expression for error dynamics $\dot{e}_i$ from (1.14) and simplifying the expression for $\dot{V}_i$ can be written as follows

$$\begin{aligned}\dot{V}_i &= \beta_i e_i\, \tilde{W}_i^T \Phi_i(X) + \beta_i e_i \epsilon_i - \beta_i k_{\tau_i} e_i^2 \\ &- \frac{\tilde{W}_i^T \dot{\hat{W}}_i}{\gamma_i} - \dot{\hat{W}}_i \left[\frac{\partial \Phi_i}{\partial X}\right] \theta \left[\frac{\partial \Phi_i}{\partial X}\right]^T \tilde{W} \\ &+ \tilde{W}^T \frac{d}{dt}\left[\frac{\partial \Phi_i}{\partial X}\right] \theta \left[\frac{\partial \Phi_i}{\partial X}\right]^T \tilde{W} \end{aligned} \tag{1.19}$$

Collecting the coefficients of $\tilde{W}$ and equating it to zero the following weight update rule in continuous time is obtained

$$\dot{\hat{W}} = \beta_i e_i \left(\frac{I_p}{\gamma_i} + \left[\frac{\partial \Phi_i}{\partial X_i}\right] \Theta_i \left[\frac{\partial \Phi_i}{\partial X_i}\right]^T\right)^{-1} \phi(X_i) + \left(\frac{I_p}{\gamma_i} + \left[\frac{\partial \Phi_i}{\partial X_i}\right] \Theta_i \left[\frac{\partial \Phi_i}{\partial X_i}\right]^T\right)^{-1} \times \frac{d}{dt}\left(\frac{\partial \Phi_i}{\partial X}\right) \Theta \left(\frac{\partial \Phi_i}{\partial X}\right)^T \tilde{W} \tag{1.20}$$

The weight update rule (1.20) involves the term $\tilde{W}$ on RHS of the expression, i.e to propagate the weight matrix it is required to have the information of term $\tilde{W}_k = W_k - \hat{W}_k$ which in turn demands information on the ideal weights at all time step 'k'. Since the ideal weights are not available direct information of the term $\tilde{W}$ cannot be extracted. Having said that the information of the difference of the ideal weights and actual weight can be extracted from the difference of the actual disturbance term $d(X)$ and approximated disturbance term $\hat{d}(X)$. It is quite evident that the actual disturbance term $d(X)$ is unavailable for computation, hence an estimate of the actual disturbance term obtained through the Extended Kalman Filter (EKF) is used instead of the actual disturbance term $d(X)$ in the above expression for the estimate of the term $\tilde{W}$ the details of which are given in subsequent section.

The term $\tilde{W}$ can be obtained from definition of the term $\phi^T \tilde{W}$ as follows

$$\phi^T \tilde{W} = (d_{est}(X) - \hat{d}(X)) \tag{1.21}$$

note that the actual disturbance term is replaced by the EKF estimate of the $d(X)$, this approximation is reasonable, since the estimate of $d(X)$ can be represented in terms of ideal weights as $d_{est}(X) = W^T \Phi(X_{est})$. Multiplying through out by the term ϕ and rewrite the above equation (1.21) as

$$\phi^T \phi \tilde{W} = \phi(d_{est}(X) - \hat{d}(X)) \tag{1.22}$$

Distribution Code A: Approved for public release, distribution is unlimited

simplifying the above equation the expression for the term $\tilde{W}$ is obtained as follows

$$\tilde{W} = (\phi^T \phi)^{-1} \phi (d_{est}(X) - \hat{d}(X)) \tag{1.23}$$

The term $\phi^T \phi$ is positive definite scalar function hence the inverse always exists, substituting for $\tilde{W}$ in (1.20) the revised weight update rule is obtained as follows.

$$\begin{aligned} \dot{\hat{W}} &= \beta_i e_i \left(\frac{I_p}{\gamma_i} + \left[\frac{\partial \Phi_i}{\partial X_i} \right] \Theta_i \left[\frac{\partial \Phi_i}{\partial X_i} \right]^T \right)^{-1} \phi(X_i) + \left(\frac{I_p}{\gamma_i} + \left[\frac{\partial \Phi_i}{\partial X_i} \right] \Theta_i \left[\frac{\partial \Phi_i}{\partial X_i} \right]^T \right)^{-1} \times \\ & \frac{d}{dt} \left(\frac{\partial \Phi_i}{\partial X} \right) \Theta \left(\frac{\partial \Phi_i}{\partial X} \right)^T \times (\phi^T \phi)^{-1} \phi (d_{est}(X) - \hat{d}(X)) \end{aligned} \tag{1.24}$$

$$\begin{aligned} \dot{\hat{W}} &= \beta_i e_i \left(\frac{I_p}{\gamma_i} + \left[\frac{\partial \Phi_i}{\partial X_i} \right] \Theta_i \left[\frac{\partial \Phi_i}{\partial X_i} \right]^T \right)^{-1} \phi(X_i) + \left(\frac{I_p}{\gamma_i} + \left[\frac{\partial \Phi_i}{\partial X_i} \right] \Theta_i \left[\frac{\partial \Phi_i}{\partial X_i} \right]^T \right)^{-1} \times \frac{d}{dt} \left(\frac{\partial \phi}{\partial X} \right) \Theta \left(\frac{\partial \phi}{\partial X} \right)^T \times \\ & (\phi^T \phi)^{-1} \phi ((\dot{X}_{est} - \hat{f}(X) - bU) - \hat{d}(X)) \end{aligned} \tag{1.25}$$

The left over terms from Lyapunov derivative $\dot{V}_i$ equation are

$$\dot{V}_i = \beta_i e_i \epsilon_i - k_{\tau_i} \beta_i e_i^2 \tag{1.26}$$

Using $\dot{V}_i < 0$ leads to a condition

$$|e_i| > \frac{|\epsilon_i|}{k_{\tau_i}} \tag{1.27}$$

Therefore, if the network weights are updated based of the rule given in (1.25), then the identification happens as long as absolute error is greater than $\frac{|\epsilon_i|}{k_{\tau_i}}$. By increasing k_{τ_i} error bound can be theoretically reduced.

1.2 Generalized Model Predictive Static Programming

In this section, the detailed description of GMPSP algorithm is presented. General form of non-linear state dynamics and output equation is defined as,

$$\dot{X}(t) = f(X(t), U(t)) \tag{1.28}$$

Distribution Code A: Approved for public release, distribution is unlimited

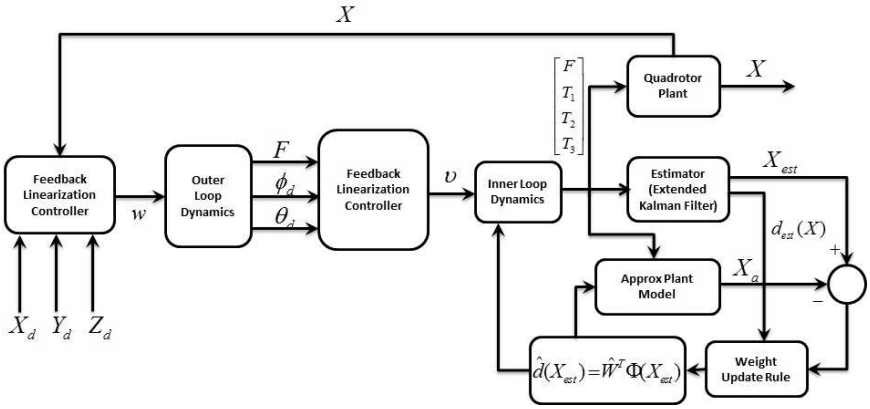

Figure 1.1: Feedback Linearization Trajectory control Augmented with RBF-NN, control Algorithm

$$Y(t) = h(X(t)) \tag{1.29}$$

Where $X \in \Re^n, U \in \Re^m$ and $Y \in \Re^p$ With known boundary conditions $X(t_0) = X_0$ and $Y_d(t_f)$ as desired output.

The philosophy of GMPSP technique is to use error history between present and desired state value and update control history. A guess control history is required to start GMPSP algorithm which yields inaccurate state solution. Error history is computed with the help of desired solution and inaccurate solution of states. This error history is use in update continuously control history until the convergence criteria is met i.e., $Y(t_f) \rightarrow Y^*(t_f)$.

Next, mathematical formulation of the GMPSP algorithm is presented, Let the error between present and desired output at the final time t_f be defined as follows,

$$\delta Y(X(t_f)) = [Y(t_f) - Y^*(t_f)] \tag{1.30}$$

By multiplying both sides of (1.28) by a weighting matrix $W(t)$ produces

$$W(t)\dot{X} = W(t)f(X(t), U(t)) \tag{1.31}$$

where, the computation of the matrix $W(t) \in \Re^{p \times n}$ is described later (1.36) in this section.

Distribution Code A: Approved for public release, distribution is unlimited

By integrating both sides of (1.31) from t_0 to t_f leads to,

$$\int_{t_0}^{t_f} [W(t)(\dot{X})(t)]dt = \int_{t_0}^{t_f} [W(t)f(X(t),U(t))]dt \tag{1.32}$$

Next, on adding the quantity $Y(X(t_f))$ to both sides of (1.32) and by using algebraic manipulation, the following is obtained,

$$Y(X(t_f)) = Y(X(t_f)) + \int_{t_0}^{t_f} [W(t)f(X(t),U(t))]dt - \int_{t_0}^{t_f} [W(t)\dot{X}(t)]dt \tag{1.33}$$

Using the integration by parts in the last term of the right hand side of (1.33) , the following can be written:

$$\begin{aligned} Y(X(t_f)) = Y(X(t_f)) - [W(t_f)X(t_f)] + [W(t_0)X(t_0) \\ + \int_{t_0}^{t_f} [W(t)f(X(t),U(t)) + \dot{W}(t)X(t)]dt \end{aligned} \tag{1.34}$$

By taking the first variation of the both sides of (1.34),

$$\begin{aligned} \delta Y(X(t_f)) = \left[\left(\frac{\partial Y(X(t))}{\partial X(t)} - W(t)\right)\delta X(t)\right]_{t=t_f} \\ + \int_{t_0}^{t_f} \left(W(t)\frac{\partial f(X(t),U(t))}{\partial X(t)} + \dot{W}(t)\right)\delta X(t)d(t) \\ + [W(t_0)\delta X(t_0)] + \int_{t_0}^{t_f} \left(W(t)\frac{\partial f(X(t),U(t))}{\partial U(t)}\right)\delta U(t)d(t) \end{aligned} \tag{1.35}$$

Next, it is desired to determine the variations $\delta Y(X(t_f))$ produced by the given $\delta U(t)$. The idea is to choose $W(t)$ in such a way that vanishes the coefficients of $\delta X(t)$ in the above equation. Weighting matrix $W(t)$ can be selected as,

$$\dot{W}(t) = -W(t)\left(\frac{\partial f(X(t),U(t))}{\partial X(t)}\right) \tag{1.36}$$

Distribution Code A: Approved for public release, distribution is unlimited

$$W(t_f) = \frac{\partial Y(X(t_f))}{\partial X(t_f)} \tag{1.37}$$

Initial condition is known Hence, the expression $\delta X(t_0) = 0$ holds true . Furthermore, substituting (1.36) and (1.37) into (1.35) produces,

$$\delta Y(X(t_f)) = \int_{t_0}^{t_f} [B_s(t)\delta U(t)]\,dt \tag{1.38}$$

Where,

$$B_s(t) = W(t)\frac{\partial f(X(t), U(t))}{\partial U(t)} \tag{1.39}$$

For optimal control formulation, cost function is defined as,

$$J' = \frac{1}{2}\int_{t_0}^{t_f} [(U^p(t) - \delta U(t))^T R(t)(U_p(t) - \delta U(t))]\,dt \tag{1.40}$$

where, $R(t) > 0$ is the non-singular matrix. The cost function in (1.40) needs to be minimized, subjected to the constraint in (1.38). With the application of optimization theory Bryson and Ho [1975], static constrained optimization problem can be formulated by using Equations (1.38) and (1.40). The augmented cost function is given as,

$$\begin{aligned} J = \frac{1}{2}\int_{t_0}^{t_f} [(U^p(t) - \delta U(t))^T R(t)(U_p(t) - \delta U(t))]\,dt \\ + \lambda^T [\delta Y(t_f) - \int_{t_0}^{t_f} [B_s(t)\delta U(t)]\,dt] \end{aligned} \tag{1.41}$$

Where, λ is the Lagrange multiplier. First variation of (1.41) leads to,

$$\delta J = -\int_{t_0}^{t_f} [R(t)(U^p(t) - \delta U(t)) + (B_s(t))^T \lambda \delta(\delta U(t))] \tag{1.42}$$

From (1.42) it is clear that a minimum of J occurs if the following expression holds true:

$$\delta U(t) = (R(t))^{-1}(B_s(t))^T \lambda + U^p(t) \tag{1.43}$$

Distribution Code A: Approved for public release, distribution is unlimited

Substituting (1.43) into (1.38) leads to

$$\delta Y(t_f) = A_\lambda \lambda + b_\lambda \tag{1.44}$$

Where,

$$A_\lambda \triangleq \left[\int_{t_0}^{t_f} \left[B_s(t)(R(t))^{-1} B_s^T(t) \right] dt \right] \tag{1.45}$$

and

$$b_\lambda \triangleq \left[\int_{t_0}^{t_f} \left[B_s(t) U^p(t) \right] dt \right] \tag{1.46}$$

By assuming that A_λ is a non-singular matrix, the following expression is obtained from (1.44)

$$\lambda = (A_\lambda)^{-1} \left[\delta Y(t_f) - b_\lambda \right] \tag{1.47}$$

substituting which into (1.43) produces

$$\delta U(t_f) = (R(t))^{-1} (B_s(t))^T \left[(A_\lambda)^{-1} \left[\delta Y(t_f) - b_\lambda \right] \right] + U^p(t) \tag{1.48}$$

Hence, the updated control is given by,

$$U(t) = -(R(t))^{-1} (B_s(t))^T \left[(A_\lambda)^{-1} \left[\delta Y(t_f) - b_\lambda \right] \right] \tag{1.49}$$

The closed form solution of control history $U(t)$ is obtained using GMPSP algorithm. The basic mechanism behind GMPSP technique is to convert the dynamic optimal control problem into a constrained static optimization problem and update the control history using small dimension weighting matrix update (1.36). This leads to fast computation of control history. Due to fast convergence property GMPSP algorithm can be applied for online applications.

Distribution Code A: Approved for public release, distribution is unlimited

2 Autonomous Soft Landing of Quadrotor

Owing to highly agile nature of the quadrotor vehicle and inherent existence of exogenous disturbing forces, safe landing of the quadrotor with safe approach velocities is always a tricky and critical issue for safety of the vehicle and surroundings. Landing scenario becomes still more critical when safe landing is to be achieved on the specified location within a confined space with obstacles. For a non qualified pilot, safe landing of the vehicle is a challenging task to accomplish. External disturbances like cross wind, blade flapping, ground effect on thrust variation due to downwash vehicle dynamics change according to possible flight scenarios. Apart from the external factors measurement noise also hinders safe decent through error in position and attitude measurement of the vehicle. Vision-based methods for aerial vehicles to detect navigation targets have been used recently and reported in literature to identify the targets for path following and landing. Brockers et al. Brockers et al. [2011] have presented Autonomous landing and ingress of micro-air-vehicles in urban environments using monocular vision processing. Templeton et al. Templeton et al. [2007] demonstrated a model-predictive flight control system using a monocular camera. 3D feautures are tracked in earth fixed inertial frame to estimate elevation and appearance of the structure, their approach assumes the availability of GPS information for computation. Recently Blosch et al. Blosch et al. [2010] highlight in their work the use of a monocular vision-based SLAM algorithm for accurate determination of the pose of a UAV in GPS denied environments. This work, while not exploring techniques landing site selection per se, dwells more towards the nonlinear controller and online adaptive disturbance estimation techniques augmenting the capability

Distribution Code A: Approved for public release, distribution is unlimited

of operating UAV systems in all types of environments and concentrate on the autonomous landing capability of the vehicle. For simulations, the problem statement of landing at location $X = 5m, Y = 5m$ and $Z = 0.05m$ assumed to be identified by available ranging techniques is used. The vehicle is assumed to be hovering above ground level at $Z = 10m$ a error in initial condition in X and Y direction is assumed, the vehicle is off by 1m in each direction that is $X = 4m, Y = 4m$. From this initial position of the quadrotor the controller is designed to achieve auto-landing at predetermined location, under the influence of external disturbance of rotor blade flapping, propeller axis misalignment. The control architecture and simualtion results are presented in the further section.

2.1 Quadrotor- Plant Dynamics

This section provides the details of kinematics and dynamic equation of motion of the rigid body quadrotor. The notation and the co-ordinate frames used are typical in aeronautics literature, for further details one can refer Beard [2008]. Euler angles in sequence of 1-2-3 (Roll ϕ, Pitch θ and Yaw ψ) is used for deriving the transformation matrix for translation and angular velocity for the vehicle. This chosen frame for transformation has advantage that it renders the outer-loop control i.e. position control independent of yaw attitude of the vehicle. Quadrotor Dynamics equation of motion is expressed as follows

$$\begin{aligned} \ddot{\xi} &= -G + \frac{1}{M} R_t F \qquad (2.1) \\ \ddot{\varphi} &= -R_r^{-1} J^{-1} \left(R_r \dot{\varphi} \times J R_r \dot{\varphi} \right) \\ &- R_r^{-1} \left(\frac{\partial R_r}{\partial \theta} \dot{\theta} + \frac{\partial R_r}{\partial \psi} \dot{\psi} \right) \dot{\varphi} \\ &+ R_r^{-1} J^{-1} T + d_{external}(X) \end{aligned}$$

(2.2)

where rotation matrices for transforming translation and angular position of the Quadrotor from body frame to inertial frame are as follows

$$R_t = \begin{bmatrix} C_\theta C_\psi & -C_\theta S_\psi & S_\theta \\ S_\phi S_\theta C_\psi + C_\phi S_\psi & -S_\phi S_\theta S_\psi + C_\phi C_\psi & -S_\phi C_\theta \\ -C_\phi S_\theta C_\psi + S_\phi S_\psi & C_\phi S_\theta S_\psi + S_\phi C_\psi & C_\phi C_\theta \end{bmatrix}$$

Distribution Code A: Approved for public release, distribution is unlimited

$$R_r = \begin{bmatrix} C_\psi C_\theta & S_\psi & 0 \\ -S_\psi C_\theta & C_\psi & 0 \\ S_\theta & 0 & 1 \end{bmatrix}$$

and vectors $\xi = \left[x, y, z\right]^T$ and $\varphi = \left[\phi, \theta, \psi\right]^T$ are position and angle vector of the quadrotor in inertial frame of reference. $V = [u, v, w]^T$ and $\Omega = \left[p, q, r\right]^T$ are translation velocity and rotation velocity in body fixed reference frame and $G = \left[0, 0, g\right]^T$ denotes gravity vector. Interested readers can refer Beard [2008], Lee et al. [2011] and references there in for the detailed derivation of the equation of motion of the Quadrotor dynamics.

2.1.1 Quadrotor Blade Flapping Phenomenon

A quadrotor UAV in linear translational flight experiences a aerodynamic effect known as "Blade Flapping Phenomenon". This aerodynamic phenomenon causes disturbing moments acting about the c.g of the vehicle. The disturbing moments are caused as the result of the unequal lifting forces experienced by the rotor blade due the variation in the free stream velocity experienced by the leading edge and trailing edge of the rotor blade. In steady state this effect causes a steady bias in the rotor blade angle causing tilt in thrust vector and a component of the trust vector parallel to Roll-pitch plane causes the moments acting at the c.g of the vehicle. The steady bias in the rotor blade tilt due blade flapping phenomenon also causes a steady moment due structural deflection of the blade, this effect is observed in the more stiff propellers, the reaction moment at the rotor hub is product of the stiffness coefficient of the rotor blade and deflection caused due to flapping.

The tilt of the rotor plane through angle ξ_ϕ in pitch and ξ_θ in roll directions, generates a thrust vector component in longitudinal and lateral directions causing disturbing moments about pitch and roll axis,

$$M_{pitch} = Thsin\xi_\phi + K_\beta \xi_\phi \tag{2.3}$$

$$M_{roll} = Thsin\xi_\theta + K_\beta \xi_\theta \tag{2.4}$$

Distribution Code A: Approved for public release, distribution is unlimited

where T is total thrust (N), h is the perpendicular distance between rotor plane and roll-pitch plane passing through c.g of the vehicle and ξ_ϕ, ξ_θ are the rotor plane deflection angles.
The rotor plane deflection angle is function of the translation velocities of the vehicle w.r.to the free stream of air in inertial frame and roll and pitch attitude angular rates of the quadrotor vehicle and can be evaluated as follows

$$\xi_\phi = C_1 \dot{x} + C_2 \dot{\phi} \tag{2.5}$$

$$\xi_\theta = C_1 \dot{y} + C_2 \dot{\theta} \tag{2.6}$$

where C_1 and C_2 are aerodynamic constants depending on the rotor blade properties. Full analysis of the blade flapping phenomenon is beyond the scope of this paper, interested reader can refer Huang et al., Hoffmann et al. and references there in for further details.

2.2 Neuro-Adaptive Dynamic Inversion for Quadrotor Control

The baseline controller is evaluated using dynamics inversion method Lee et al. [2011]. The Guidance/Outer loop dynamics concerns the position control of the vehicle. The linear feedback representation of outer-loop system dynamics can be written as

$$\ddot{\xi} = w$$

Linear control technique such as linear quadratic regulator (LQR) is used to evaluate the control w. Control w is of form $w = -K_{position}(\xi - \xi_d)$. Now using synthetic controller w the total thrust vector is evaluated as follows

$$w = -G + \frac{1}{M} R_t F \tag{2.7}$$

denoting $U = R_t F$ from above equation U can be expressed as $U = Mw + MG$ using the definition $U = R_t F$ the expression for total thrust F is solved as follows

$$F = \sqrt{(U_1^2 + U_2^2 + U_3^2)}$$

Distribution Code A: Approved for public release, distribution is unlimited

and desired roll and pitch attitude is evaluated as follows

$$\phi_d = -sgn(U_2)cos^{-1}\left(\sqrt{\frac{U_3^2}{U_2^2+U_3^2}}\right)$$

and

$$\theta_d = -sgn(U_1)cos^{-1}\left(\sqrt{\frac{U_2^2+U_3^2}{U_1^2+U_2^2+U_3^2}}\right)$$

Desired yaw angle is considered to be $\psi_d = 0$. The desired attitude angles forms input to the innerloop controller of the quadrotor.

Similarly the inner loop dynamics can be written in linear form for the feedback linearization controller evaluation as follows.

$$\begin{aligned} T &= JR_r\left(\nu + R_r^{-1}J^{-1}\left(R_r\dot{\varphi}\times JR_r\dot{\varphi}\right)\right) \\ &+ JR_r\left(R_r^{-1}\left(\frac{\partial R_r}{\partial\theta}\dot{\theta}+\frac{\partial R_r}{\partial\psi}\dot{\psi}\right)\dot{\varphi}+\hat{d}(X)\right) \end{aligned} \tag{2.8}$$

2.3 Extended Kalman Filter(EKF) Estimate of the Quadrotor State Vector

The quadrotor state vector is available through the sensor measurement. On-board sensors like three axis accelerometers and rate gyro provides the body rate information with respect to the body frame and GPS measures the position, ground speed and course angle with respect to inertial frame. Rate gyros and accelerometers output body rate information and is assumed to be corrupted by zero mean measurement noise and process noise arising due to blade flapping phenomenon, hence a EKF estimate needs to be propagated for information on the attitude state vectors. Where as the position and velocity of the quadrotor in inertial frame is assumed to be faithfully available through GPS measurement. Hence the EKF is only implemented for the inner-loop dynamics, there-by with directly available outerloop state information the EKF estimate of inner loop state vector forms the complete state information of the quadrotor vehicle. Fig 2.1 provides details to EKF philosophy implementation for quadrotor state estimation, for further details interested readers can refer Crassidis and Junkins [2011]. The estimate of the uncertainty, derived from EKF estimate of the innerloop state vectors for

Distribution Code A: Approved for public release, distribution is unlimited

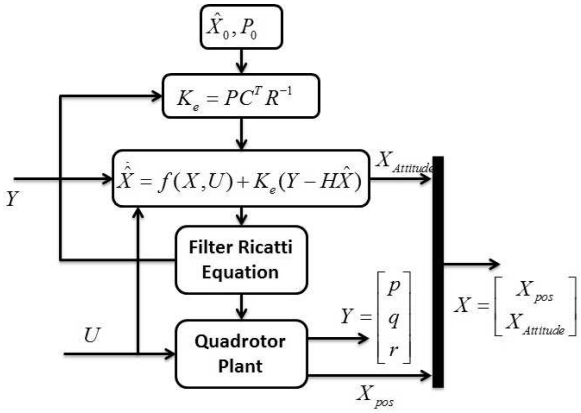

Figure 2.1: Extended Kalman Filter Implementation for Partial State Estimation (Inner Loop Attitude State Estimates)

weight update rule (1.20) is evaluated as follows

$$\hat{d}(X_{est}) = \dot{X}_{est} - f_0(X) - g(X)U \tag{2.9}$$

2.4 Numerical Simulation for Quadrotor Landing

The estimate of the uncertainty, derived from EKF estimate of the innerloop state vectors for weight update rule (1.20) is evaluated as follows

$$\hat{d}(X_{est}) = \dot{X}_{est} - f_0(X) - g(X)U \tag{2.10}$$

2.4.1 Simulation Results

This section presents simulation results for quadrotor Landing control. The control law designed treats the disturbing moment due to aerodynamic effect of blade flapping phenomenon as un-modeled uncertainty term which is captured online through RBF-NNs. Outer loop control is achieved through a dynamic inversion control and inner loop attitude control is achieved through the online adapted dynamic inversion control. At low speeds and less aggressive maneuver the aerodynamic effects due quadrotor blade flapping phenomenon are less sever

Distribution Code A: Approved for public release, distribution is unlimited

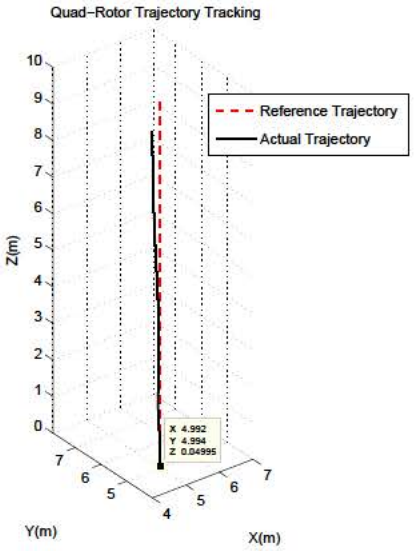

Figure 2.2: Quad Rotor following the pre Defined Trajectory: Reference Trajectory, Actual and Approximate trajectory of vehicle

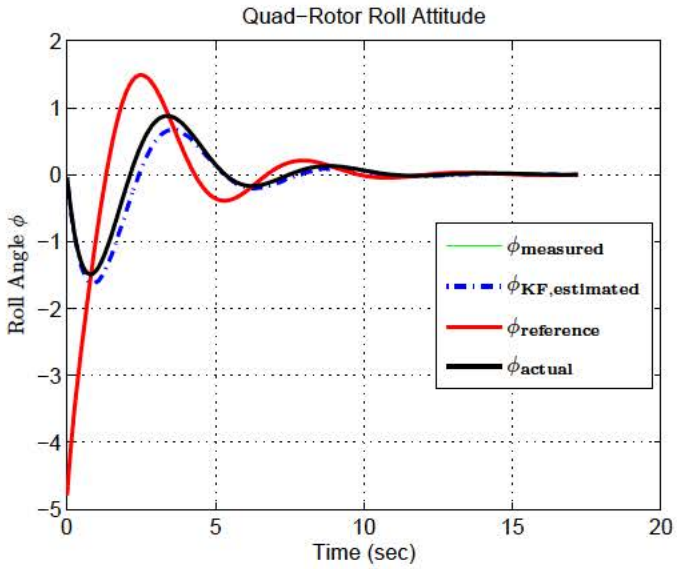

Figure 2.3: Reference/Desired, Actual, Measured and Kalman filter Estimate of the Roll Attitude of the Quad

Distribution Code A: Approved for public release, distribution is unlimited

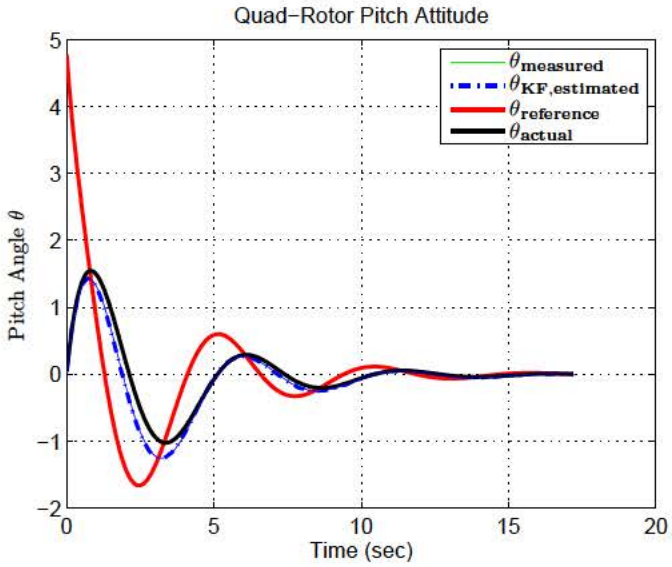

Figure 2.4: Reference/Desired, Actual, Measured and Kalman filter Estimate of the Pitch Attitude of the Quad

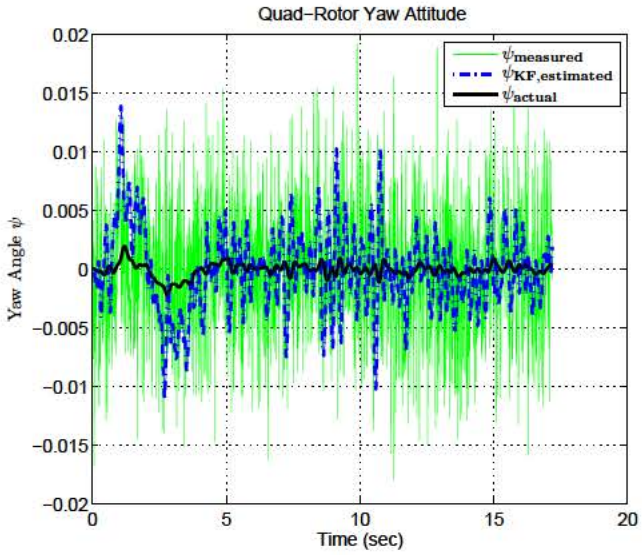

Figure 2.5: Reference/Desired, Achieved Yaw Attitude of the Quad

Distribution Code A: Approved for public release, distribution is unlimited

and it is seen that a well tuned PID controller is sufficient for satisfactory command tracking In

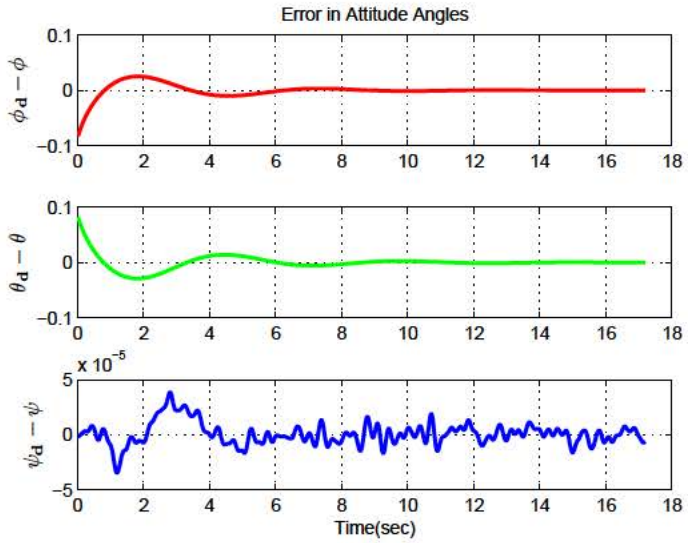

Figure 2.6: Error in Attitude Angle of the Quadrotor

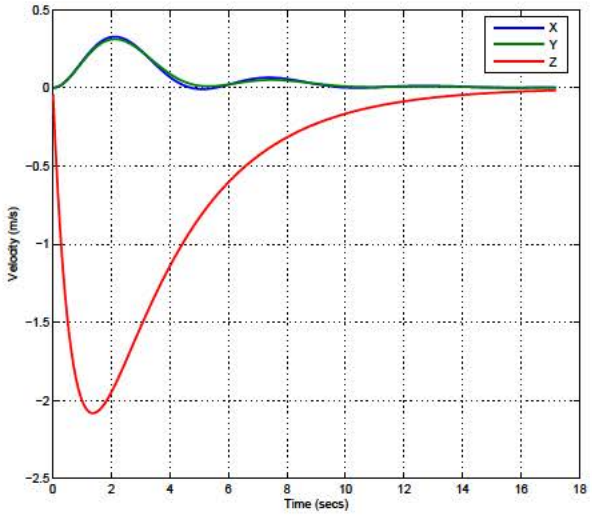

Figure 2.7: Quad Rotor following the pre Defined Trajectory: Reference Trajectory, Actual and Approximate trajectory of vehicle

translational flights it is observed that at larger speeds the blade flapping causes a considerable amount of disturbing moment at the c.g of the vehicle. At higher speeds the restoring forces may not be sufficient and vehicle eventually becomes unstable unless the control architecture

Distribution Code A: Approved for public release, distribution is unlimited

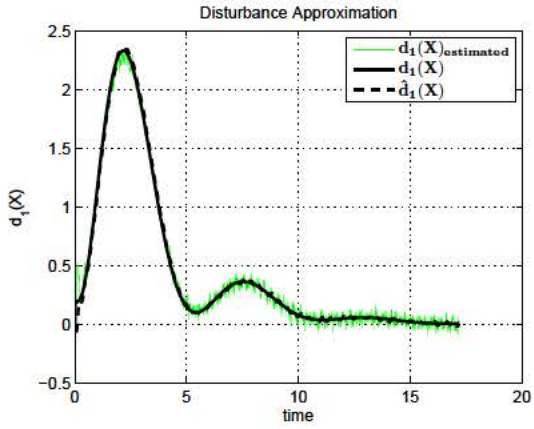

Figure 2.8: Disturbance in Channel 1, Actual, Approximated, Kalman Filter Estimated

implemented takes into account the blade flapping phenomenon. The performance of the proposed controller in auto-landing of the vehicle from altitude of $10m$ is shown in the Fig 2.2. The desired location of the landing is $X = 5m$, $Y = 5m$ and $Z = 0.05m$. The vehicle initial condition at point of start of decent for landing is considered t be at $X = 4m$, $Y = 4m$ and $Z = 10m$ above ground level. Quadrotor roll attitude against the desired commanded attitude is shown in the Fig 2.3. Figure 2.3 also gives the details of the measured attitude angle and EKF estimate of the roll attitude of the vehicle.

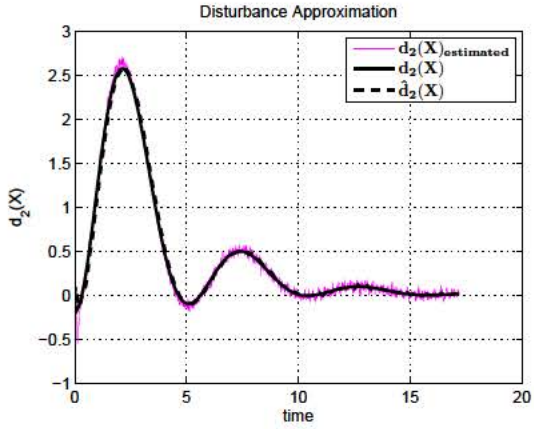

Figure 2.9: Disturbance in Channel 3, Actual, Approximated, Kalman Filter Estimated

Similarly Fig 2.4,2.5 gives the details of the attitude control of the quadrotor in pitch and yaw axis respectively. It is observed that despite the influence of the disturbing aerodynamic

Distribution Code A: Approved for public release, distribution is unlimited

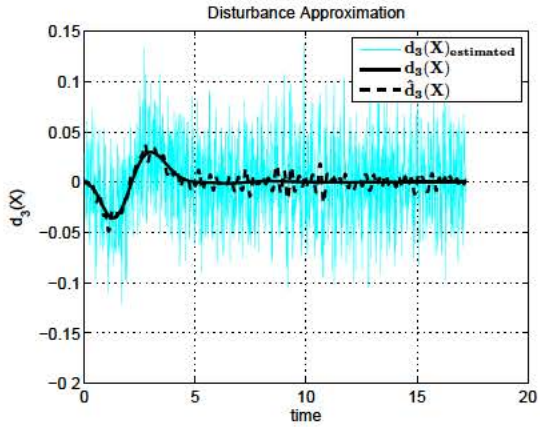

Figure 2.10: Disturbance in Channel 3, Actual, Approximated, Kalman Filter Estimated

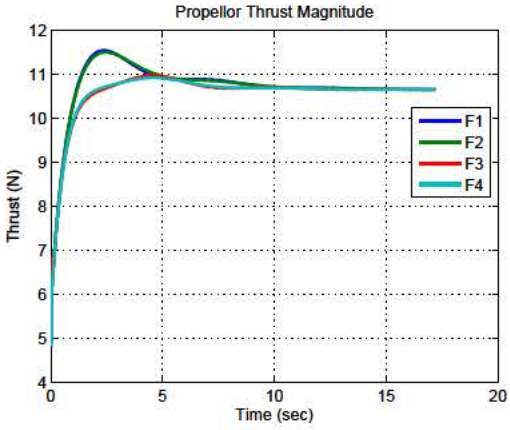

Figure 2.11: Control,Thrust Produced by four propellers

moments the perfect trajectory tracking is achieved. The vehicle attitude follows the desired attitude angles with high accuracy, the errors in the attitude angles is presented in Fig 2.6. The plot of state history for the commanded trajectory following in X, Y and Z in inertial frame of reference, are provided in the Fig 2.2.

The performance of the three RBF-NN in approximating the disturbance terms in each channel is given by the Fig 2.8,2.9 and 2.10. Figure 2.8,2.9 and 2.10 provides the details of the actual disturbing moments, EKF estimated disturbance and neural network approximate of the uncertainty arising due to blade flapping phenomenon. It can be observed that EKF estimation of $d(X)$ through estimation of acceleration term $\dot{X}_{est}$ leads to amplification of the effect of the sensor noise into the uncertainty estimate. Authors wishes to highlight the notable

Distribution Code A: Approved for public release, distribution is unlimited

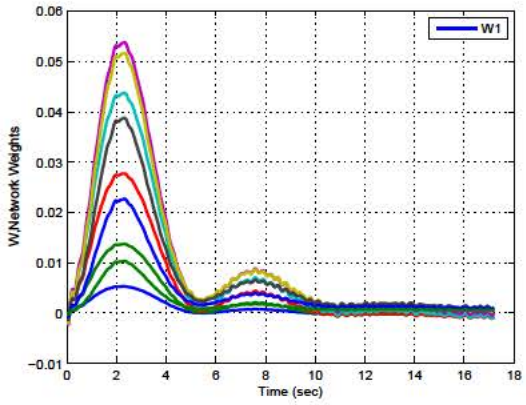

Figure 2.12: Weight history, W1

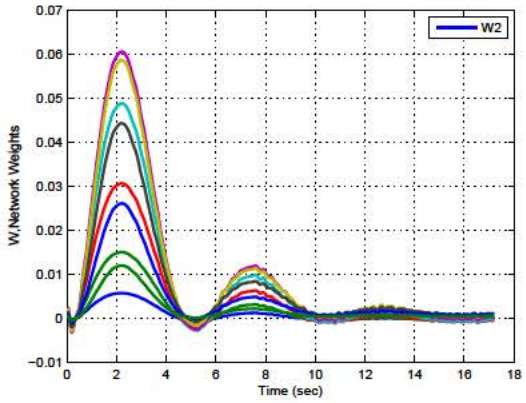

Figure 2.13: Weight history, W2

advantage of weight update rule presented in this paper, using the noisy EKF estimate of the uncertainty into the weight update rule (1.25) a precise approximation is achieved through the neural network approximation for unknown system dynamics. Figure 2.11 provides the details of the final control effort needed in terms of the propeller thrust to achieve the commanded trajectory tracking. The control effort F_1, F_2, F_3, F_4 corresponds to thrust generated by front, right, back and left propellers respectively. Figure 2.12, 2.13 provides time history plot of the weight propagation for online approximation of the uncertainty. The value of weight W_3 are negligible since the disturbance in yaw axis is zero hence the plot is not provided.

Distribution Code A: Approved for public release, distribution is unlimited

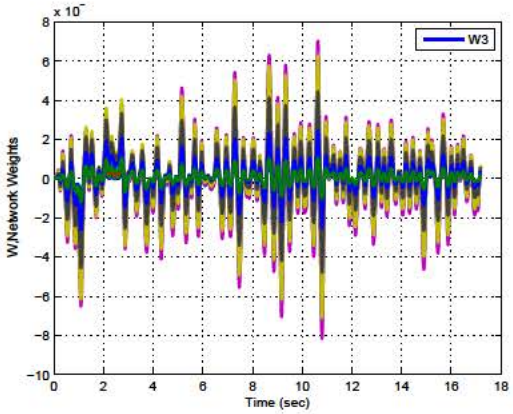

Figure 2.14: Weight history, W3

Distribution Code A: Approved for public release, distribution is unlimited

3 Autonomous Soft Landing of Lunar Module

The powered descent phase starts from perilune as the nearest point from the Moon surface. During the powered descent phase the reverse thrust action provides a braking mechanism to reduce the high orbital velocity (about $1700 m/s$) of the spacecraft. At the end of the powered descent phase the spacecraft is positioned very close to the lunar surface about $200 m$ altitude with a reduced velocity in the range of $(0-20)$ m/s.

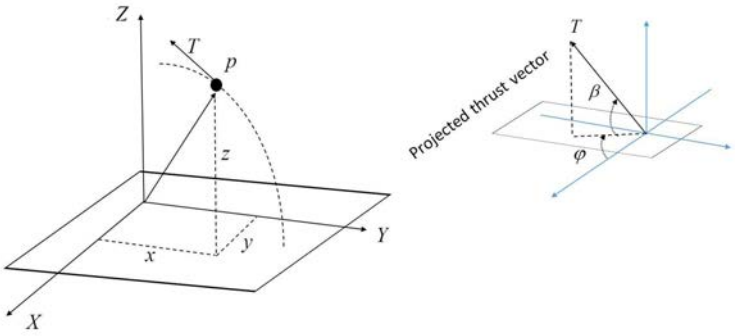

Figure 3.1: Landing site based frame of reference

3.1 Problem Statement

Due to the uneven terrain of lunar surface, the visual sensors are used to detect a suitable landing site. It might be necessary to shift the landing site from the nominal location to a nearby smooth ground. The operation of switching the landing site is known as re-targeting.

Distribution Code A: Approved for public release, distribution is unlimited

Hence it is necessary to obtained an on board guidance law that can ensure the soft landing requirement while accounts for the correction of nominal landing site. An analytical guidance law for fuel optimal planetary landing was studied in D'Souza [1997]. A close form expression of optimal commanded acceleration has been obtained for the spacecraft equation of motion in terms of current position and velocities and also a function of the time-to-go parameter. The guidance law is popular as constrained terminal velocity guidance (CTVG). A relations between the CTVG with the classical proportional navigation (PN), zero effort velocity miss (ZEVM) and zero effort miss(ZEM) feedback guidance laws are presented in Guo et al. [2011]. The CTVG guidance ensures the soft landing but fails to demonstrate the vertical orientation of the spacecraft during the terminal descent. A modified CTVG guidance considers the derivative of the acceleration command as a virtual input vector. The terminal attitude-constrain is incorporated in the modified CTVG law, is presented in Zhao et al. [2014]. The computation of the modified time to go presented in Zhao et al. [2014] is a very complex recursive relation. Authors have investigated the numerical method for the optimal control design for the lunar landing. Zhang Jianhui Jianhui et al. [2011] uses the Chebyshev pseudo-spectral method for optimal control design using two dimensional planar motion of lunar module. Time scaling transformation followed by Control vector parameterization is presented in Gao et al. [2013], Liu et al. [2008] as trajectory optimization method for the planner dynamics of lunar module. Although the various numerical optimal control methods are studied for optimal guidance of lunar modules,few are suitable for onboard implementation due to poor computational efficiency with low convergence rate.

G-MPSP is a numerical optimal control algorithm deals with general non-linear systems. The algorithm is based on the philosophies of the approximate dynamic programming and nonlinear model predictive control. The formulation of G-MPSP converts the dynamic optimization problem (in HJB framework) into a static programming problem results a close form solution for the control update history. The close form control update law makes the G-MPSP computationally efficient. The fast convergence rate makes it compatible for on-board optimal guidance design. In this report G-MPSP guidance is formulated for the accurate soft landing of a lunar module. From the mission point of view, the module starting from the altitude about $200m$ requires to touchdown with near zero velocity about $2m$ altitude from the designated

Distribution Code A: Approved for public release, distribution is unlimited

landing site (determined by the vision sensor) on lunar surface. For a spacecraft with variable thrust engine,G-MPSP generates the acceleration vector (both magnitude and direction) that minimizes the fuel requirement and ensures the accurate soft landing of the module.

3.2 Spacecraft Dynamics for Lunar Mission

The spacecraft equation of motion derived in the landing site based inertial frame of reference is described as,

$$\dot{x} = u \tag{3.1}$$

$$\begin{aligned}
\dot{y} &= v \\
\dot{z} &= w \\
\dot{u} &= \frac{\mu x}{\left(x^2+y^2+z^2\right)^{3/2}} + \frac{T}{m}\cos\beta cos\varphi \\
\dot{v} &= \frac{\mu y}{\left(x^2+y^2+z^2\right)^{3/2}} + \frac{T}{m}\cos\beta\sin\varphi \\
\dot{w} &= \frac{\mu x}{\left(x^2+y^2+z^2\right)^{3/2}} + \frac{T}{m} sin\beta \\
\dot{m} &= -\frac{T}{I_{sp}g_0}
\end{aligned} \tag{3.2}$$

where, (x, y, z) topple represents the instantaneous position of the spacecraft in the inertial frame of reference. u, v and w denotes the velocity component of the module. The thrust engine is mounted on the spacecraft body, T/m describes the acceleration vector generated using the thrust engine. The direction of the thrust vector in 3-D space is represented by the angle β and φ. During the terminal descent the objective is to guide the spacecraft from an altitude of about $200m$ to the designated location on the lunar surface. The lunar gravity parameter μ is constant for the domain of operation. The initial position and the velocity of the spacecraft is considered as, $\left(x_{0,}y_{0,}z_{0,}u_{0,}v_{0,}w\right)$. The specific impulse of the thrust engine is represented by I_{sp} and g_0 is the Earth gravitational acceleration.

Distribution Code A: Approved for public release, distribution is unlimited

3.3 Fuel Optimal Guidance

The guidance objective is to obtain the thrust vector (both magnitude and direction) T, β and φ such that the consumption of the fuel mass is minimized. so the cost function J_1 is defined as,

$$J_a = \frac{m_0}{m_f} \tag{3.3}$$

The initial mass of the spacecraft m_0 is known and constant. Hence the minimization of J_a is equivalent of maximization of the spacecraft landed mass. The minimization of J_a is mathematically equivalent to minimization of the following ,

$$J_b = \ln J_a = \ln\left(\frac{m_0}{m_f}\right) \tag{3.4}$$

Using the mass dynamics given in (3.1) the above expression can be represented as,

$$\ln\left(\frac{m_0}{m_f}\right) = -\int_0^{t_f}\left(\frac{d(\ln m(t))}{dt}\right)dt$$

$$J_b = -\int_0^{t_f}\left(\frac{\dot{m}}{m}\right)dt \tag{3.5}$$

By using (3.1) , (3.5) leads to,

$$J_b = \frac{1}{I_{sp}}\int_0^{t_f}\left(\frac{T}{m}\right)dt \tag{3.6}$$

Now the acceleration components can be written as,

Distribution Code A: Approved for public release, distribution is unlimited

$$
\begin{aligned}
a_x &= \frac{T}{m}\cos\beta cos\varphi \\
a_y &= \frac{T}{m}\cos\beta\sin\varphi \\
a_z &= \frac{T}{m} sin\beta
\end{aligned} \tag{3.7}
$$

by substituting a_x, a_y and a_z in (3.6) one can obtain,

$$
J_b = \int_0^{t_f} \sqrt{a_x^2 + a_y^2 + a_z^2}\, dt \tag{3.8}
$$

here, J_b is a convex function with respect to a_x, a_y and a_z. Minimization of J_b is equivalent to minimization of

$$
J = \int_0^{t_f} \left(a_x^2 + a_y^2 + a_z^2\right) dt \tag{3.9}
$$

Therefore,maximization of the spacecraft mass of the lunar module during landing is ensured by minimizing (3.9), which results into minimization of fuel consumption during terminal descent phase.

3.4 Results and Discussion

The numerical values, considered for the simulation purpose are given as below. The nominal values of the initial state variables are considered as, $x_0 = 0m$, $y_0 = 0m$, $z_0 = 200m$ represents the initial position of the module with respect to the landing site frame of reference. $u_0 = 5m/\sec$, $v_0 = -5m/\sec$ and $w_0 = 5m/\sec$ describes the initial velocity. The initial mass of the module at perilune $M_0 = 523.5kg$. The objective is to generate the thrust vector such that the module can land safely on a designated landing site determined using the visual sensors. At the end of the terminal descent the state variables are required to be obtained as,

Distribution Code A: Approved for public release, distribution is unlimited

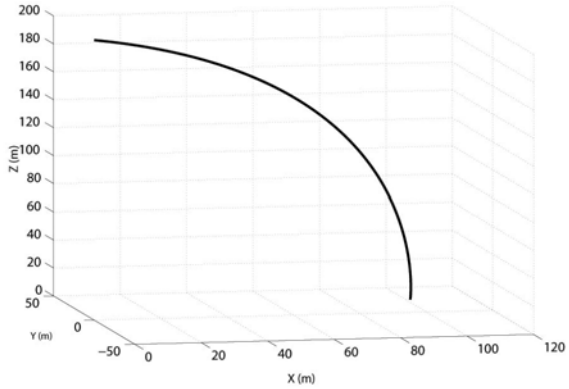

Figure 3.2: Spacecraft trajectory

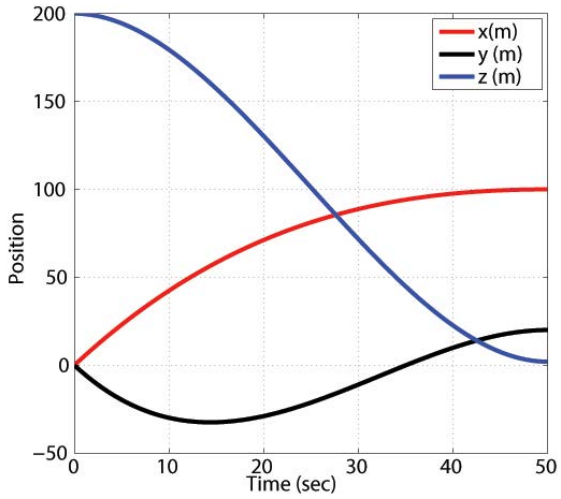

Figure 3.3: Position co-ordinate of the lunar module

$x_f = 100m$, $y_f = 20m$ and $z_f = 0m$ (the co-ordinate of the detected landing site in the same inertial frame of reference). $u_f = 0m/\sec$, $v_f = 0m/\sec$ and $w_f = 0m/\sec$ denotes the terminal touch down velocity. The lunar gravity parameter $\mu = 4.90278 \times 10^3 km^3/\sec^2$, $I_{sp} = 315\sec$. Control weight matrix $R_k(t)$ is selected as a time varying matrix to ensure the vertical landing of the module. The G-MPSP based terminal descent guidance generates the optimal commanded thrust for the lunar module. Fig.3.2 and Fig.3.3 shows the spacecraft (point mass) trajectory is starting from the specified initial position and follows a smooth curve and approaches towards the detected landing site. At the final flight time the distance of the lunar module from the ground surface is about $z - z_f = 2$. At the altitude of $2m$, the thrust engine of

Distribution Code A: Approved for public release, distribution is unlimited

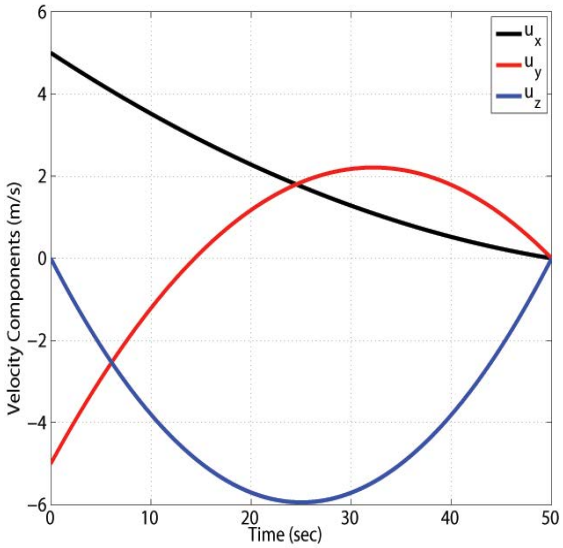

Figure 3.4: Velocity components of the lunar module

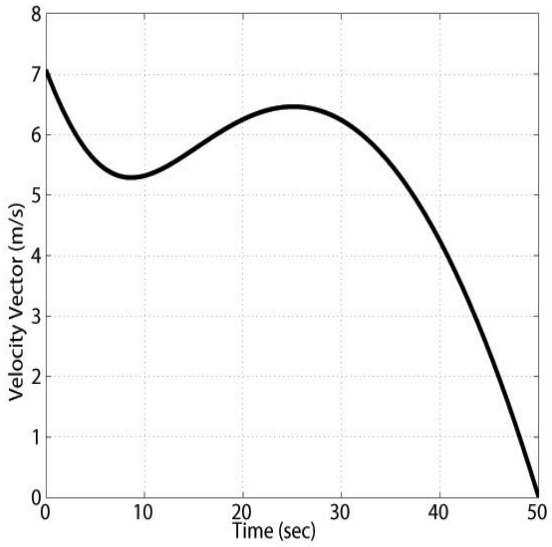

Figure 3.5: Velocity vector of the lunar module

the spacecraft remains switch off. Hence from $2m$ altitude the spacecraft will be allowed to free fall until it touches the ground. The $2m$ margin is necessary while the spacecraft touches the lunar surface, as the thrust engine plume can make a dusty environment over the solar panels mounted on the lunar module. To ensure the soft landing as the time approaches, the spacecraft velocity approaches zero as shown in Fig.3.4 and Fig.3.5. Starting from a near zero

Distribution Code A: Approved for public release, distribution is unlimited

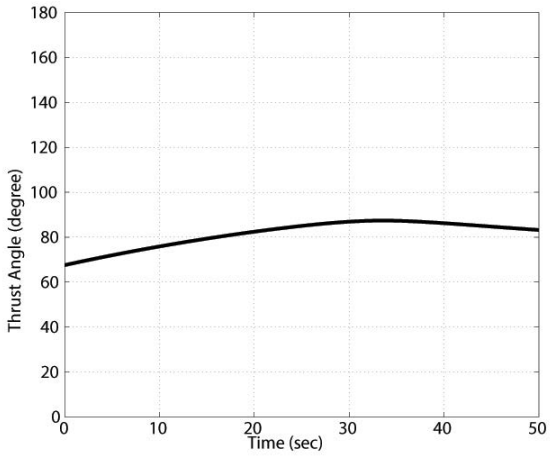

Figure 3.6: Thrust direction $beta$ profile

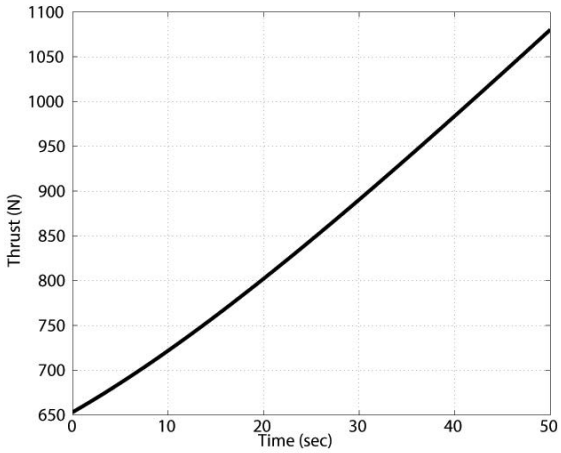

Figure 3.7: Thrust magnitude profile

initial guess control history the guidance algorithm takes four to five iterations to converge. The optimal commanded thrust vector generated using G-MPSP guidance for the variable thrust engine is shown in the Fig.3.7 and Fig.3.6.

Distribution Code A: Approved for public release, distribution is unlimited

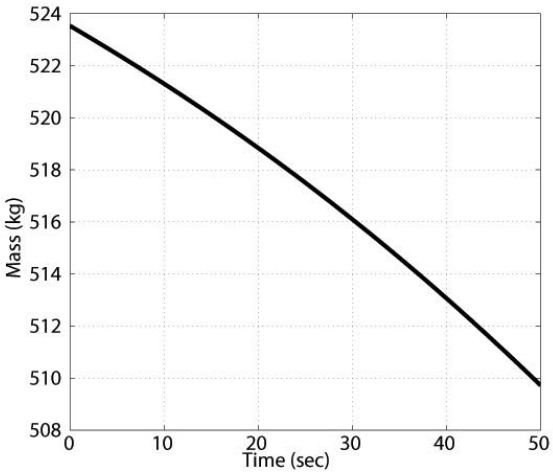

Figure 3.8: Variation spacecraft total mass

The variation of the spacecraft mass is shown in Fig.3.8, the fuel requirement during the terminal descent phase is about $14kg$.

Distribution Code A: Approved for public release, distribution is unlimited

4 CONCLUSION

Tow problems are investigated in this report. First, the autonomous guidance of soft landing for an UAV is presented. In presence of atmosphere with the utility of the aerodynamic advantage the quadrotor landing on the flat earth surface is demonstrated with a neuro-adaptive tracking control approach for autonomous landing. The approach leads to fast learning of the disturbance function in the system dynamics and with lesser transients. The presented adaptive control was experimented with quad-rotor autonomous landing problem in presence of aerodynamics uncertainty. It has been shown that the proposed approach could satisfactorily capture the uncertainty. The inner-loop neuro-adaptive dynamic inversion controller forms a very robust controller and is demonstrated to be tracking the desired attitude angles with high accuracy in presence of unmodeled dynamics and measurement sensor noise. As a result the outer-loop controller is able to perfectly track the commanded trajectory.

The second problem deals with the autonomous soft landing of a lunar module. In absence of atmosphere, where the aerodynamic advantages are not present (which is true for moon), the terminal descent of the autonomous guidance for a spacecraft on the flat moon surface is demonstrated using the recently developed G-MPSP algorithm. The proposed G-MPSP guidance ensures the objective of the spacecraft soft landing along with the minimum propellant consumption with high terminal accuracy. With the proper choice of the control weight matrix the terminal vertical orientation of the spacecraft is obtained in the soft constraint framework. The effectiveness of the proposed algorithm has been demonstrated using simulation results.

Distribution Code A: Approved for public release, distribution is unlimited

Bibliography

Randal W Beard. Quadrotor dynamics and control. *Brigham Young University*, 2008.

Michael Blosch, Stephan Weiss, Davide Scaramuzza, and Roland Siegwart. Vision based mav navigation in unknown and unstructured environments. In *Robotics and automation (ICRA), 2010 IEEE international conference on*, pages 21–28. IEEE, 2010.

Samir Bouabdallah, Pierpaolo Murrieri, and Roland Siegwart. Towards autonomous indoor micro vtol. *Autonomous Robots*, 18(2):171–183, 2005.

Roland Brockers, Patrick Bouffard, Jeremy Ma, Larry Matthies, and Claire Tomlin. Autonomous landing and ingress of micro-air-vehicles in urban environments based on monocular vision. In *SPIE Defense, Security, and Sensing*, pages 803111–803111. International Society for Optics and Photonics, 2011.

A. E. Bryson and Y. C. Ho. *Applied Optimal Control.* Hemisphere Publishing Corporation, 1975.

Girish Chowdhary, Tongbin Wu, Mark Cutler, Nazim Kemal Ure, and Jonathan How. Experimental results of concurrent learning adaptive controllers. In *AIAA Guidance, Navigation, and Control Conference (GNC),(Minneapolis, MN), AIAA*, 2012.

John L Crassidis and John L Junkins. *Optimal estimation of dynamic systems.* CRC press, 2011.

Christopher D'Souza. An optimal guidance law for planetary landing. In *Proceedings of the AIAA conference on Guidance, Navigation, and Control*, pages 1376–1381, LA, U.S.A, July 1997.

Zachary T Dydek, Anuradha M Annaswamy, and Eugene Lavretsky. Adaptive control of

Distribution Code A: Approved for public release, distribution is unlimited

quadrotor uavs in the presence of actuator uncertainties. *AIAA Infotech@ Aerospace*, pages 20–22, 2010.

Xiangyu Gao, Lili Shao, and Hao Liu. An exact penalty function method for optimal lunar soft landing control problem. In *2013 32nd Chinese Control Conference (CCC)*, pages 2215–2220, 2013.

Yanning Guo, Matt Hawkins, and Bong Wie. Optimal feedback guidance algorithms for planetary landing and asteroid intercept. In *Proceedings of the AAS/AIAA Astrodynamics Specialist Conference*, number AAS 11-588, Alaska, July 2011.

Robert F Hartley, François Hugon, Pat Anderson, and Hever Moncayo. Development and flight testing of a model based autopilot library for a low cost unmanned aerial system. 2013.

Gabriel M Hoffmann, Haomiao Huang, Steven L Waslander, and Claire J Tomlin. Quadrotor helicopter flight dynamics and control: Theory and experiment. In *Proc. of the AIAA Guidance, Navigation, and Control Conference*, volume 2, 2007.

Haomiao Huang, Gabriel M Hoffmann, Steven Lake Waslander, and Claire J Tomlin. Aerodynamics and control of autonomous quadrotor helicopters in aggressive maneuvering. In *Robotics and Automation, 2009. ICRA'09. IEEE International Conference on*, pages 3277–3282. IEEE, 2009.

Jianhui, Zhang, and Qi bo Peng. Lunar soft landing trajectory optimization by a chebyshev pseudospectral method. In *2011 IEEE International Conference on Computer Science and Automation Engineering (CSAE)*, volume 2, pages 425–430, 2011.

Girish Joshi and Radhakant Padhi. Robust satellite formation flying using dynamic inversion with modified state observer. In *Control Applications (CCA), 2013 IEEE International Conference on*, pages 568–573. IEEE, 2013.

Sang-hyun Lee, Seung Hoon Kang, and Youdan Kim. Trajectory tracking control of quadrotor uav. In *Control, Automation and Systems (ICCAS), 2011 11th International Conference on*, pages 281–285. IEEE, 2011.

Xing-Long Liu, Guang-Ren Duan, and Kok-Lay Teo. Optimal soft landing control for moon lander. *Automatica*, 44(4):1097–1103, 2008.

Distribution Code A: Approved for public release, distribution is unlimited

Paul Pounds, Robert Mahony, and Peter Corke. Modelling and control of a large quadrotor robot. *Control Engineering Practice*, 18(7):691–699, 2010.

Todd Templeton, David Hyunchul Shim, Christopher Geyer, and S Shankar Sastry. Autonomous vision-based landing and terrain mapping using an mpc-controlled unmanned rotorcraft. In *Robotics and Automation, 2007 IEEE International Conference on*, pages 1349–1356. IEEE, 2007.

Mario Valenti, Brett Bethke, Gaston Fiore, Jonathan P How, and Eric Feron. Indoor multi-vehicle flight testbed for fault detection, isolation, and recovery. In *Proceedings of the AIAA Guidance, Navigation, and Control Conference and Exhibit, Keystone, CO*, volume 63, page 64, 2006.

Brian T Whitehead and Stefan R Bieniawski. Model reference adaptive control of a quadrotor uav. In *AIAA Guidance, Navigation, and Control Conference*, pages 2–5, 2010.

Dang-Jun Zhao, Bing-Yan Jiang, and Xin-Guang Lv. Terminal attitude-constrained optimal feedback guidance for pinpoint planetary landing. In *2nd IAA Conference on Dynamics and Control of Space Systems*, number IAA-AAS-DyCoSS2-14 -15-04, Roma, Italy, March 2014.

Distribution Code A: Approved for public release, distribution is unlimited